Microporous and Mesoporous Materials 181 (2013) 74–82

Contents lists available at ScienceDirect

Microporous and Mesoporous Materials

journal homepage: www.elsevier.com/locate/micromeso

Efficiency of zeolite MCM-22 with different SiO_2/Al_2O_3 molar ratios in gas phase glycerol dehydration to acrolein

Camila S. Carriço [a], Fernanda T. Cruz [a], Maurício B. Santos [a], Heloise O. Pastore [b], Heloysa M.C. Andrade [a,c], Artur J.S. Mascarenhas [a,c,*]

[a] Laboratório de Catálise e Materiais, Departamento de Química Geral e Inorgânica, Instituto de Química, Universidade Federal da Bahia, R. Barão do Jeremoabo, s/n, Ondina, 40170-280 Salvador, Bahia, Brazil
[b] Grupo de Peneiras Moleculares Micro- e Mesoporosas, Instituto de Química, Universidade Estadual de Campinas, CP 6154, 13083-970 Campinas, SP, Brazil
[c] Instituto Nacional de Ciências e Tecnologia em Energia e Ambiente (INCT – E&A), Universidade Federal da Bahia, R. Barão do Jeremoabo, s/n, Ondina, 40170-280 Salvador, Bahia, Brazil

ARTICLE INFO

Article history:
Received 16 April 2013
Received in revised form 17 June 2013
Accepted 13 July 2013
Available online 20 July 2013

Keywords:
MCM-22
Dehydration of glycerol
Sustainable production of acrolein

ABSTRACT

The gas-phase dehydration of glycerol was conducted over MCM-22 zeolite with different SiO_2/Al_2O_3 molar ratios. MCM-22 zeolites were synthesized and characterized by XRD, FTIR, TG, SEM, EDX, textural analysis by N_2 physisorption and NH_3-TPD. The MCM-22 zeolites have presented good crystallinity, high surface areas and a decreased amount of acid sites and strength with increasing SiO_2/Al_2O_3 ratio was observed. The glycerol conversion and acrolein selectivity increased with increasing reaction temperature from 280 °C to 320 °C on MCM-22 (30) catalyst. As long as the concentration of glycerol solution was in the range from 10% to 36.6%, there was no noticeable difference in the glycerol conversion but the acrolein yield increased with water amount in the feed. The glycerol conversion and selectivity to acrolein at 320 °C using glycerol feed of 36.6% during 10 h of reaction decreased in the following order: MCM-22 (30) > MCM-22 (50) > MCM-22 (80). This result shows that glycerol dehydration to acrolein is strongly dependent on the acid sites density and external surface area of the zeolite MCM-22.

© 2013 Elsevier Inc. All rights reserved.

1. Introduction

MCM-22 was first synthesized and patented in 1990 by researchers from Mobil Oil Corporation [1] and the Structure Commission of the International Zeolite Association (IZA) designated this peculiar topology as MWW (Mobil Twenty Two). This zeolite crystallizes as a lamellar precursor which condenses to a full three-dimensional structure under calcination, with crystals having hexagonal morphology and axis c- unit cell perpendicular to the surface [2].

MCM-22 structure consists of two independent pore systems: one of these systems consists of two-dimensional sinusoidal channels defined by 10-membered rings, whose internal diameter is 4.0 × 5.9 Å, similar to those found in zeolite ZSM-5; and the other channel system is formed by stacking supercages of 7.1 × 7.1 × 18.2 Å, accessible through 10 member rings. This peculiar porous systems allowed an efficient distribution of the acid sites so on the external surface as in the zeolite cavities [3,4].

The zeolite MCM-22 is widely used in various catalytic reactions such as disproportionation of toluene [5], aromatization of methane [6], alkylation of benzene [7], alkane cracking reactions [8], methanol-to-olefin conversion [9], and also as an additive in FCC catalysts [10] due to its acidity, which is not restricted to acid sites inside the porous systems, but also presents acid sites located in the semi cavities ("cups") on the outer surface of the crystallites [11].

Zeolites have shown excellent catalytic performance in vapor phase glycerol dehydration to acrolein, because of their tunable Brönsted and Lewis acidity and shape selectivity associated with well-defined pore size. ZSM-5 is the most studied molecular sieve in this reaction, with satisfactory conversion and acrolein selectivity, but the high acidity of this material causes an occlusion of cavity by coke deposition [12]. Higher conversion of glycerol and selectivity to acrolein are favored with catalysts with high amount of acid sites, associated with larger pore size, and therefore, MCM-22 is a promising alternative [13]. However, until this moment no scientific papers were published using MCM-22 as an acid catalyst for the gas phase dehydration of glycerol to acrolein, but a chinese patent requires that MCM-22 can be used to produce acrolein from glycerol [14].

In this work, zeolite H-MCM-22 was synthesized with SiO_2/Al_2O_3 molar ratios = 30, 50 and 80 and investigated in the vapor phase dehydration of glycerol to acrolein.

* Corresponding author at: Laboratório de Catálise e Materiais, Departamento de Química Geral e Inorgânica, Instituto de Química, Universidade Federal da Bahia, R. Barão do Jeremoabo, s/n, Ondina, 40170-280 Salvador, Bahia, Brazil. Tel.: +55 71 3283 6820; fax: +55 71 3235 5166.
E-mail address: artur@ufba.br (A.J.S. Mascarenhas).

1387-1811/$ - see front matter © 2013 Elsevier Inc. All rights reserved.
http://dx.doi.org/10.1016/j.micromeso.2013.07.020

2. Experimental

2.1. Synthesis of catalysts

MCM-22 was synthesized with different SiO_2/Al_2O_3 molar ratios = 30, 50 and 80 by the static method, adapted from the method proposed by Marques and coworkers [15]. MCM-22 (30) was prepared by the addition of 4.6 g of aluminum nitrate (Sigma–Aldrich) in an aqueous solution 0.56 mol L^{-1} of sodium hidroxide (Synth) until its total solubilization. Then, 14.9 mL of hexamethyleneimine (Sigma–Aldrich), used as structure directing agent, was added dropwise and 11 g of silica Aerosil 200 (Degussa) was added slowly, under vigorous stirring until forming a homogeneous gel. The gel was aged during 30 min under stirring and transferred to a Teflon™-coated stainless steel autoclave. The hydrothermal synthesis was conducted at 150 °C for 10 days. After filtered, the as synthesized material was ion-exchanged with 1 mol L^{-1} NH_4NO_3 (Synth) at ambient temperature for 24 h, followed by calcination in a N_2 flow at 550 °C to produce H-MCM-22 form. The synthesis of MCM-22 with SiO_2/Al_2O_3 molar ratio 50 and 80 was done similarly, except by adjusting the amounts of $Al(NO_3)_3.9H_2O$ and NaOH, in order to achieve OH^-/SiO_2 = 0.20 and 0.15, respectively, as shown in Table 1. The hydrothermal treatment duration was also adjusted to warrant good crystallinity.

2.2. Catalyst characterization

The crystal structure was confirmed by X-ray diffraction, whose XRD patterns were collected on a Shimadzu XRD-6000 unit, which operates with a CuKα radiation at a voltage of 40 kV, current of 30 mA, and graphite monochromator, in the region of 1.4–50° 2θ at a scan rate of 2° min^{-1}. Relative crystallinities of the samples were estimated by integration of the peaks in the region of 2θ = 25.5–31.2°. The FTIR spectra of the samples were collected in a Perkin Elmer Spectrum BX spectrometer using 0.1% KBr pellets, with resolution of 4 cm^{-1}, in the range of 4000–400 cm^{-1}. Thermogravimetry was conducted on a Shimadzu TGA-50 at temperatures ranging from 25 to 1000 °C with heating rate of 10 °C min^{-1} under nitrogen flow of 50 mL min^{-1} in order to verify the mass loss with increasing temperature. In order to evaluate MCM-22 morphology, micrographs of various magnifications were obtained in a Shimadzu SS-550 microscope, with an acceleration voltage of 7–15 kV after metallization with gold. The composition of different SiO_2/Al_2O_3 molar ratios was verified by elemental analysis in an energy dispersive X-ray spectrometer Shimadzu EDX-720 model and textural analysis was obtained by nitrogen physisorption at −196 °C in a Micromeritics ASAP 2020 equipment, using the BET, BJH and t-plot methods. The samples were pretreated at 350 °C for 3 h under vacuum (2 mm Hg), in order to remove any physisorbed species on the sample surface. Temperature-programmed desorption of NH_3 (NH_3-TPD) profiles were obtained in a Micromeritics Chemsorb 2720 equipped with a TCD to measure the NH_3 desorption. The samples were pretreated in He flow at 300 °C for 1 h, then cooled to ambient temperature. The NH_3 adsorption was carried out at ambient temperature in NH_3/He (9.9% mol/mol) with a flow rate of 25 mL min^{-1} for 1 h. After the chemisorption, the system was purged with He and heated until 150 °C for 1 h to eliminate physisorbed ammonia. After cooling to room temperature, the NH_3-TPD was performed by heating the sample from 30 to 600 °C at a heating rate of 10 °C min^{-1} while monitoring the TCD signal. Experimental parameters were set up in order to minimize artifacts and to enable a proper interpretation of NH_3-TPD profiles.

2.3. Catalytic test

The catalytic performance of MCM-22 zeolite with different SiO_2/Al_2O_3 molar ratios in the vapor phase glycerol dehydration to acrolein was investigated at atmospheric pressure in a continuous flow vertical reactor on borosilicate glass at the temperature range of 280–320 °C. A solution of 10–36.6 wt% glycerol in water was fed using a peristaltic pump operating at 0.033 mL min^{-1} and a N_2 flow of 30 mL min^{-1} was conducted to the reactor containing 50–300 mg of the catalyst during 10 h of reaction, depending on the desired weight/flow ratio (W/F). The bed height was kept nearly constant by dispersing the respective catalyst weight with glass beads. The condensable products were collected in a cold trap containing a 0.1% solution of hydroquinone and analyzed by a Perkin Elmer Clarus 500 gas chromatograph operating with a flame ionization detector (GC-FID) and OV-315 column (30 × 0.32 mm id). The glycerol conversion and selectivity to acrolein were quantified according to the following equations:

$$\text{Glycerol conversion}(\%) = 100 \times (n_{\text{glycerol,in}} - n_{\text{glycerol,out}})/n_{\text{glycerol,in}} \quad (1)$$

$$\text{Acrolein selectivity}(\%) = 100 \times n_{\text{acrolein,formed}}/n_{\text{glycerol,consumed}} \quad (2)$$

The formaldehyde, acetaldehyde, acrolein, propionaldehyde and acetone selectivities were confirmed by high performance liquid chromatography (HPLC) after derivatization with 2,4-dinitrophenylhydrazine. The HPLC analyses were performed on a Agilent Series 1100 model equipped with a Bruker C18 column (250 × 2.1 mm) using as mobile phase a gradient mixture of water:acetonitrile.

For comparison, ZSM-5 (SiO_2/Al_2O_3 = 30) was tested under the same conditions.

3. Results and discussion

3.1. Synthesis and characterization

The X-ray diffraction patterns showed in Fig. 1 are in good agreement with literature data for the MCM-22 [3,4,16]. The comparison of as-synthesized (Fig. 1a) and calcined (Fig. 1b) XRD patterns shows significant changes due to condensation of the lamellar precursor of the zeolite in its three-dimensional structure, with consequent increase of relative crystallinity. The increasing of the SiO_2/Al_2O_3 molar ratios results in a loss of crystallinity for as-synthesized zeolite MCM-22 as well as a change in the relative proportion between the peaks in the region of 5–10° 2θ. In the case of calcined samples, changes were observed in the relative intensities of the peaks in the regions between 20° and 23° 2θ and between 26.5° and 30° 2θ. These findings are also observed in isomorphous

Table 1
Synthesis parameters and elemental analysis for MCM-22 samples.

Sample	$NaOH/SiO_2$	HMI/SiO_2	H_2O/SiO_2	T (°C)	Time (days)	SiO_2/Al_2O_3		Relative Crystallinity (%)
						Nominal	EDX	
MCM-22 (30)	0.30	0.60	30	150	10	30	36.6	100
MCM-22 (50)	0.20	0.60	30	150	12	50	47.2	93
MCM-22 (80)	0.15	0.60	30	150	15	80	78.0	81

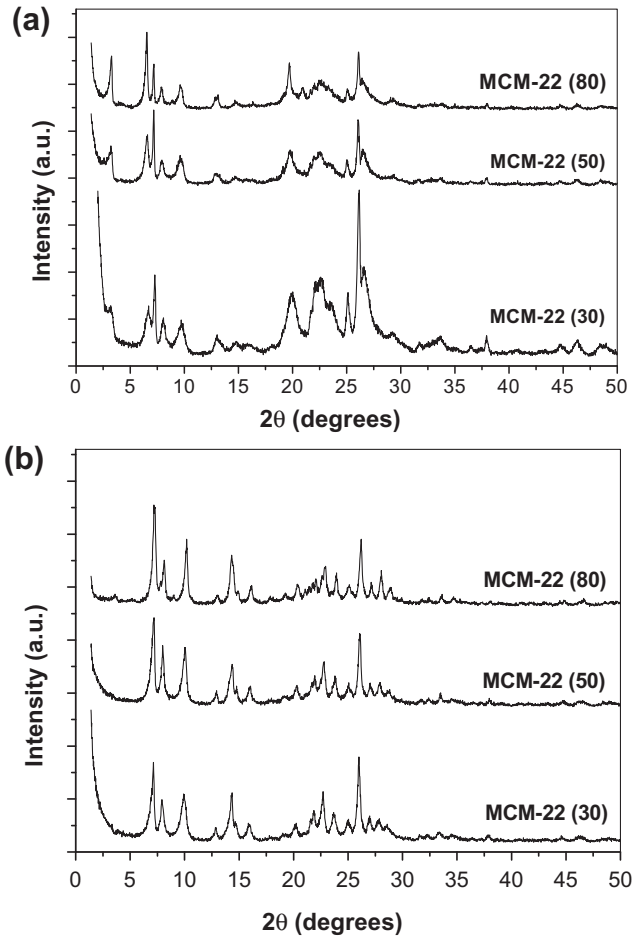

Fig. 1. X-ray powder patterns of the zeolite MCM-22 with different SiO_2/Al_2O_3 molar ratios: (a) as-synthesized and (b) calcined.

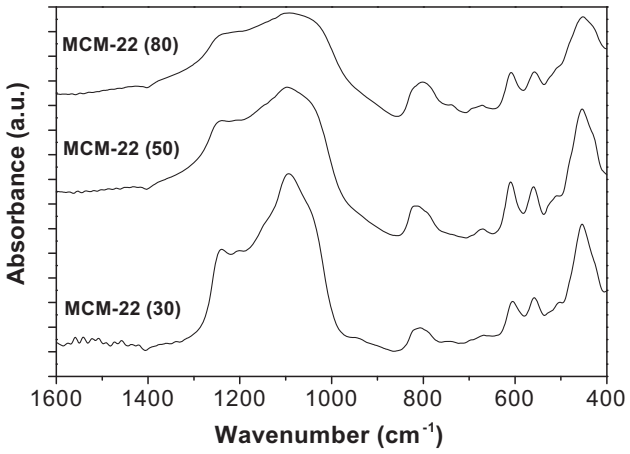

Fig. 2. FTIR spectra of MCM-22 zeolite obtained with different SiO_2/Al_2O_3 molar ratios.

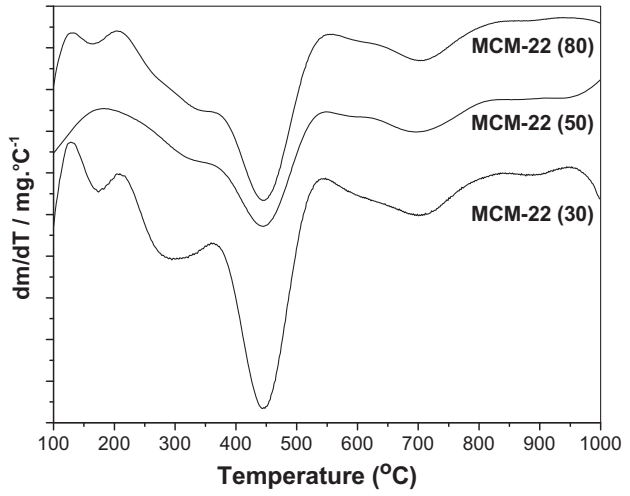

Fig. 3. Derivative thermogravimetry of MCM-22 zeolite obtained with different SiO_2/Al_2O_3 molar ratios.

ITQ-1 [17], which is the silica analogue of zeolite MCM-22, indicating that these changes are due to the lower incorporation of aluminum atoms in the structure of the aluminosilicate.

The infrared spectra of the calcined samples are shown in Fig. 2. It was possible to observe the characteristic bands of the MCM-22 at the wavelengths 1236, 1196 and 1090 cm^{-1}, corresponding to the asymmetric stretching vibration of the tetrahedron TO_4 (T = Si or Al) and 835 cm^{-1} assigned to the symmetric vibration. The bands observed at 650–550 and 400 cm^{-1}, correspond to angular deformation of the tetrahedron and double rings, respectively. These double rings are similar to those found in structures of ZSM-5 and Y zeolites [3,18].

Based on the derivative thermogravimetry curves (DTG) in Fig. 3, three events were observed: (i) loss of physisorbed water below 130 °C, (ii) loss of protonated (H^+-HMI) and non-protonated (HMI) organic template between 130 and 510 °C, and (iii) above 510 °C, desorption of hexamethyleneimine fragments. The displacement of TG curves observed for different SiO_2/Al_2O_3 molar ratios is attributed to different strengths of interactions of the directing agent (HMI) with the acid sites of zeolite [3,19].

The images obtained by scanning electron microscopy are shown in Fig. 4. The crystallites are platelet shaped with different morphologies, which are tightly assembled in toroidal particles with a small hole at the center, whose diameters varies from 10 to 13 μm [20]. This is the typical morphology observed for non-agitated MCM-22 samples. As SiO_2/Al_2O_3 molar ratio increases, platelets become more agglomerated, resulting in nearly spherical particles, similar to a "ball of wool" [21]. It was also observed that the increase of SiO_2/Al_2O_3 molar ratio resulted in a particle size decrease, as can be seen in SEM images.

The results of elemental analysis by EDX are shown in Table 1. It was observed that the values of SiO_2/Al_2O_3 molar ratios determined by EDX are in good agreement with expected values.

The MCM-22 samples exhibited type Ib adsorption isotherms (Fig. 5), typical of microporous materials [22,23]. It is also observed the presence of secondary mesopores, characterized by the hysteresis loop at high relative pressures, and an enhanced increase in the amount of adsorbed N_2 when P/Po tends to 1.0 due to multilayer adsorption on the external surface of the crystallites. Based on the textural analysis, showed in Table 2, it can be concluded that an increase in the SiO_2/Al_2O_3 ratio is accompanied by a reduction in the external area and a decrease in the volume of mesopores, probably due to the higher particle aggregation. Furthermore, the decrease in micropore volume is probably related to the lower relative crystallinity with increasing SiO_2/Al_2O_3 molar ratio.

The temperature-programmed desorption profiles, were collected using NH_3 as probe molecule, and are shown in Fig. 6, and quantitative results are summarized in Table 3. The surface acidity of the zeolites can be related to the aluminum content, so the amount of total acid sites decreases with the increase of the SiO_2/Al_2O_3 ratio [12]. Moreover, a shift of the desorption peaks to

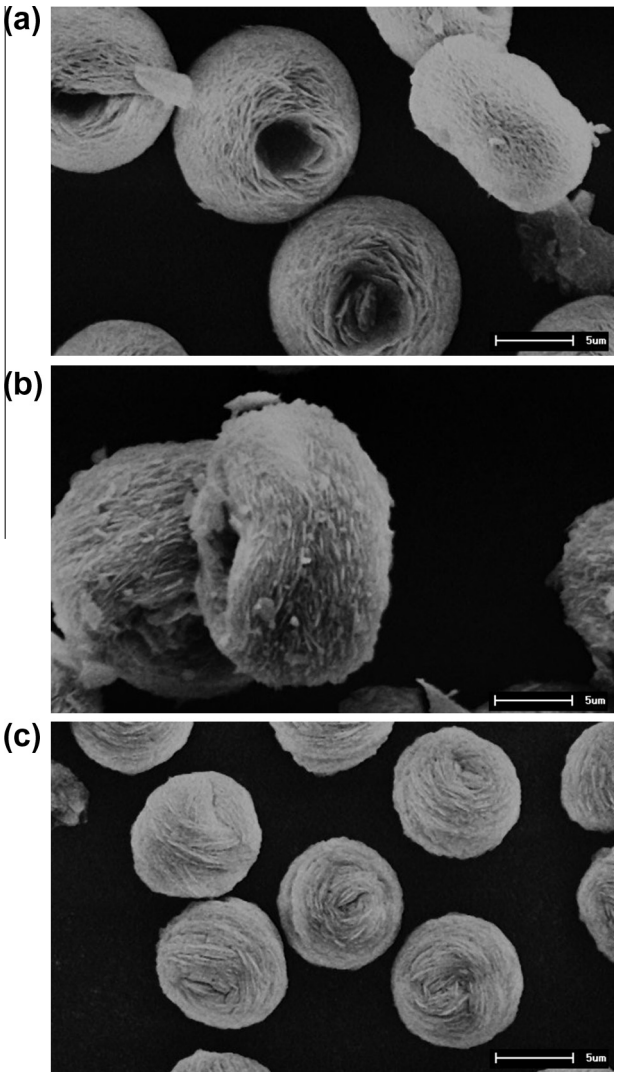

Fig. 4. SEM images of MCM-22 zeolite obtained with SiO_2/Al_2O_3 molar ratios: (a) 30, (b) 50 and (c) 80.

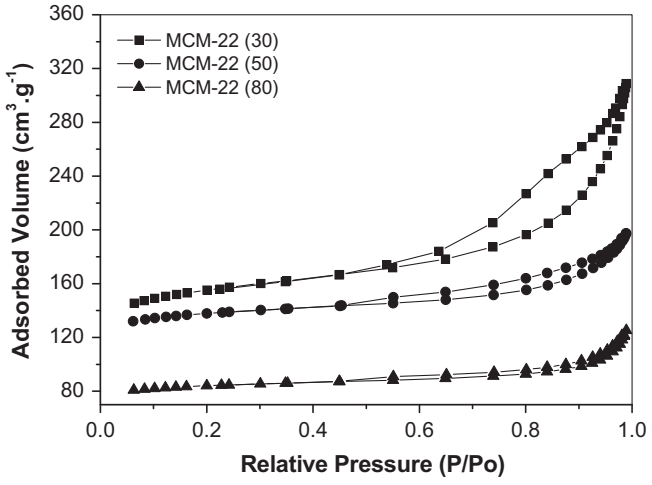

Fig. 5. Adsorption isotherms of MCM-22 zeolite with molar ratio SiO_2/Al_2O_3 (▲) 30, (●) 50 and (■) 80.

lower temperatures was observed, suggesting that weaker acid sites are present in MCM-22 with high content of aluminum.

Table 2
Textural analysis of MCM-22 zeolites.

Sample	S_{BET} ($m^2\ g^{-1}$)	S_{micro} ($m^2\ g^{-1}$)[a]	S_{ext} ($m^2\ g^{-1}$)[a]	V_{micro} ($cm^3\ g^{-1}$)[a]	V_{meso} ($cm^3\ g^{-1}$)[b]	d_{meso} (Å)[b]
MCM-22 (30)	525	381	144	0.177	0.285	99.2
MCM-22 (50)	464	381	83	0.177	0.113	86.4
MCM-22 (80)	282	235	47	0.110	0.074	108.7

[a] Determined by BET and t-plot methods.
[b] Determined by BJH method.

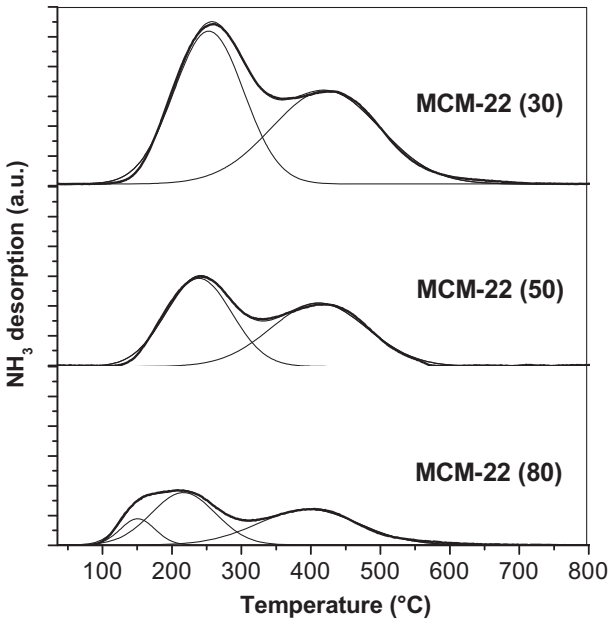

Fig. 6. The temperature-programmed desorption of NH_3 (NH_3-TPD) profile of H-MCM-22 synthesized with different SiO_2/Al_2O_3 ratios.

Table 3
Acid properties of MCM-22 catalysts.

Sample	Type of site	T_m (°C)	Density of acid sites (mmol g^{-1})	
			Partial	Total
MCM-22 (30)	Moderate	253	0.61	1.19
	Strong	421	0.58	
MCM-22 (50)	Weak	237	0.37	0.76
	Strong	416	0.39	
MCM-22 (80)	Weak	146	0.08	0.70
	Weak	211	0.30	
	Strong	395	0.32	

Some authors discussed that NH_3-TPD cannot be used to attribute acid strength, without rigorously considering confinement effects [24], because NH_3 heat of protonation/adsorption does not change significantly for different zeolite topologies [25]. Furthermore, no difference in acid strength has been noted in high silica zeolites by ^{13}C MAS NMR of adsorbed acetone [26]. However, in this work all materials have the same zeolite topology, therefore these effects can be considered constant for the different samples and the changes in NH_3-TPD profiles resulted only of SiO_2/Al_2O_3 molar ratio variation.

According to the data shown in Table 3, strong and weak acid sites are observed in almost the same relative proportion for the

samples MCM-22 (30) and MCM-22 (50). For the sample MCM-22 (80) it was observed a new type of weak acid site, probably due to sylanol Si(OH) defects.

3.2. Catalytic test

The conversion of glycerol is very high during the first hours of reaction (~100%), but decreases significantly with time on stream due to coke formation. The effects of reaction temperature, W/F ratio, glycerol content and SiO_2/Al_2O_3 molar ratio were evaluated by comparing the catalytic performance (conversion and selectivity) from 2 to 10 h.

3.2.1. Effect of the reaction temperature

The effect of the reaction temperature on the glycerol dehydration was investigated for MCM-22 (30) catalyst, as shown in Fig. 7. The glycerol conversion significantly increased with increasing reaction temperatures, but severe deactivation was observed at higher temperatures. These results are in good agreement with literature data for molecular sieves. For example, Kim et al. [12] observed that the glycerol conversion significantly increased with increasing reaction temperatures for H-ZSM-5 with molar ratio SiO_2/Al_2O_3 = 150. Selectivity increased up to 315 °C and then decrease with further increased reaction temperatures. The same behavior was observed for H-β (SiO_2/Al_2O_3 = 25) and H-ferrierite (SiO_2/Al_2O_3 = 55) [27]. Despite of the higher glycerol conversion, it was observed that at lower temperatures MCM-22 deactivates slowly by coke formation, but is less selective to acrolein, the main product of interest.

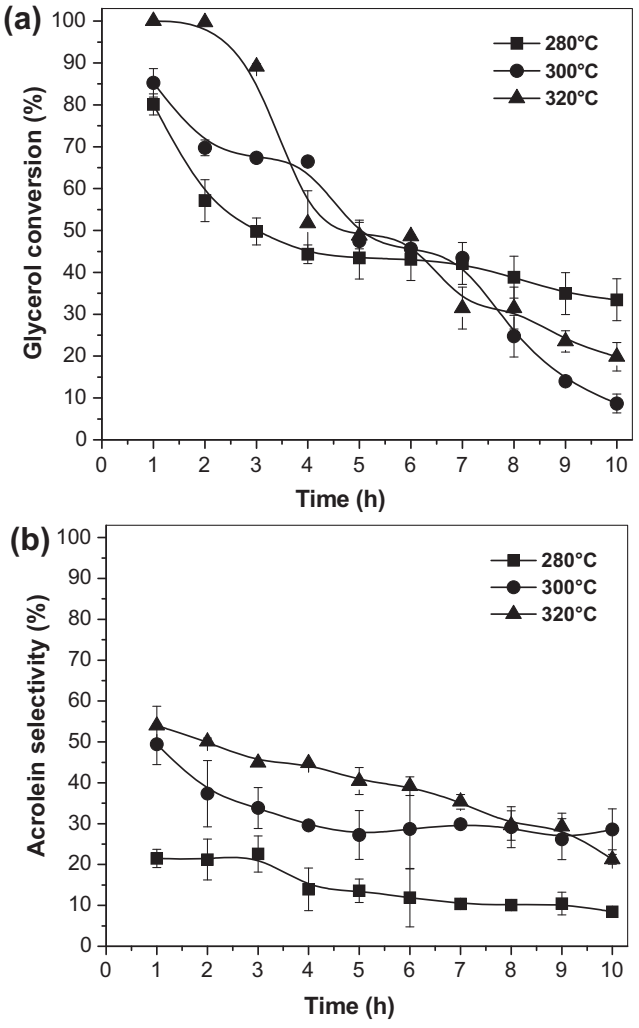

Fig. 7. Glycerol conversion and acrolein selectivity over MCM-22 (30) catalyst at different temperatures. Feed composition: 36.6% glycerol; glycerol flow = 0.33 mL/min, catalyst weight = 0.10 g.

Table 4
The catalytic performance for the dehydration of glycerol over MCM-22 catalyst with different temperatures.[a,b]

Catalyst	MCM-22 (30)		
Temperature (°C)	280	300	320
Conversion (%)	57.14 (33.45)	69.76 (8.69)	99.75 (20.20)
Acrolein yield (%)	12.13 (2.82)	26.04 (2.48)	49.92 (4.30)
Molar selectivity (%)			
Acrolein	21.22 (8.44)	37.33 (28.59)	50.05 (21.28)
1-hydroxyacetone	0.99 (0.52)	2.35 (1.84)	2.04 (0)
Formaldehyde	1.12 (0.86)	1.76 (6.07)	4.60 (13.57)
Acetaldehyde	7.86 (6.12)	3.63 (23.84)	5.53 (15.28)
Acetone	0.46 (0.14)	0.30 (0.51)	0.15 (0.39)
Allyl alcohol	0.53 (0)	0.62 (0.33)	0.27 (0)
Propionic acid	1.05 (0.54)	1.65 (1.58)	4.21 (0)
Propionaldehyde	0.21 (0.35)	0.23 (1.29)	0.11 (0.74)
Others	66.56 (83.03)	52.13 (35.95)	33.04 (48.74)
Coke[c] (%)	18.78	22.08	24.61

[a] Feed composition: 36.6% glycerol; glycerol flow = 0.33 mL/min, catalyst weight = 0.10 g.
[b] The conversion and selectivity were analyzed for the products obtained during the initial 2 h of reaction. Data in parenthesis were analyzed for the products obtained from 10 to 12 h of reaction.
[c] After the reaction for 12 h.

The product distribution in the dehydration of glycerol is shown in Table 4 for the condensate obtained after 2 and 10 h of reaction, respectively. These results show that acrolein is the main reaction product, but significant amounts of acetol (1-hydroxyacetone), formaldehyde and acetaldehyde are also formed. The formation of acetol is consistent with the mechanism of dehydration of glycerol via interaction of the Brönsted acid sites of the zeolite with the hydroxyl group bonded to a primary carbon or to Lewis acid sites [28]. The formation of formaldehyde and acetaldehyde is mainly due to thermal decomposition of acrolein.

Other minor byproducts such as acetone, allyl alcohol, propionaldehyde and propionic acid were observed. Acrylic acid and acetic acid were not formed in appreciable amounts, but they are products of acrolein oxidation, and are possibly formed by exposition to atmospheric oxygen during the sampling step.

The increased amount of byproducts at higher temperatures can be explained by the contribution of two factors: (i) the temperature increase favors the occurrence of reactions which do not occur at lower temperatures, and (ii) coke formation, which is favored at higher temperatures, modifies the nature of the active sites and favors parallel reactions [29].

Non-condensable byproducts, such as light gases (CH_4, CO, CO_2), are shown in Table 4 as "others". The selectivity to these byproducts decreases with temperature increase, because acrolein selectivity is favored, but also coke formation is more extensive.

3.2.2. Effect of W/F ratio

The effect of *W/F ratio* in glycerol dehydration to acrolein is showed in Fig. 8. The increase in W/F ratio from 20.8 to 125 g s $mmol^{-1}$ does not change the initial conversion of glycerol, but the deactivation by coke formation seems to be slower for higher W/F ratio values. MCM-22 (30) presents a conversion of nearly 65% after 10 h on stream at W/F = 125 g s $mmol^{-1}$.

The selectivity to acrolein showed a similar behavior. It was observed that higher W/F ratio favors a higher selectivity to acrolein, which suggests that glycerol conversion and acrolein selectivity strongly depend on the W/F ratio [27,30]. The glycerol conversion

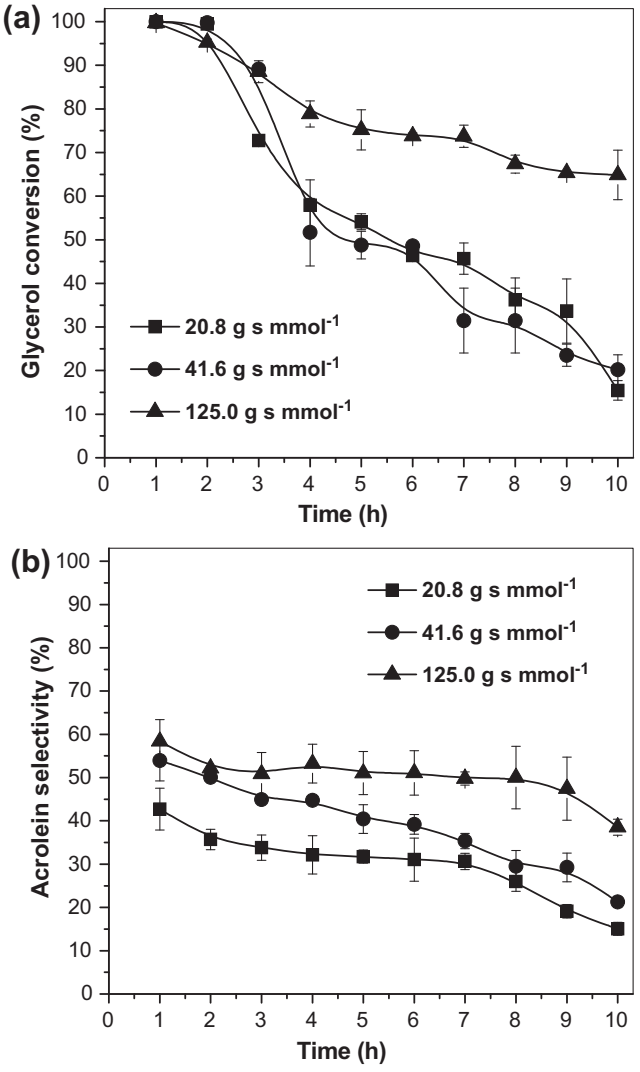

Fig. 8. Glycerol conversion and acrolein selectivity over MCM-22 (30) catalyst at different contact time. Feed composition: 36.6% glycerol, glycerol flow = 0.33 mL/min, T = 320 °C.

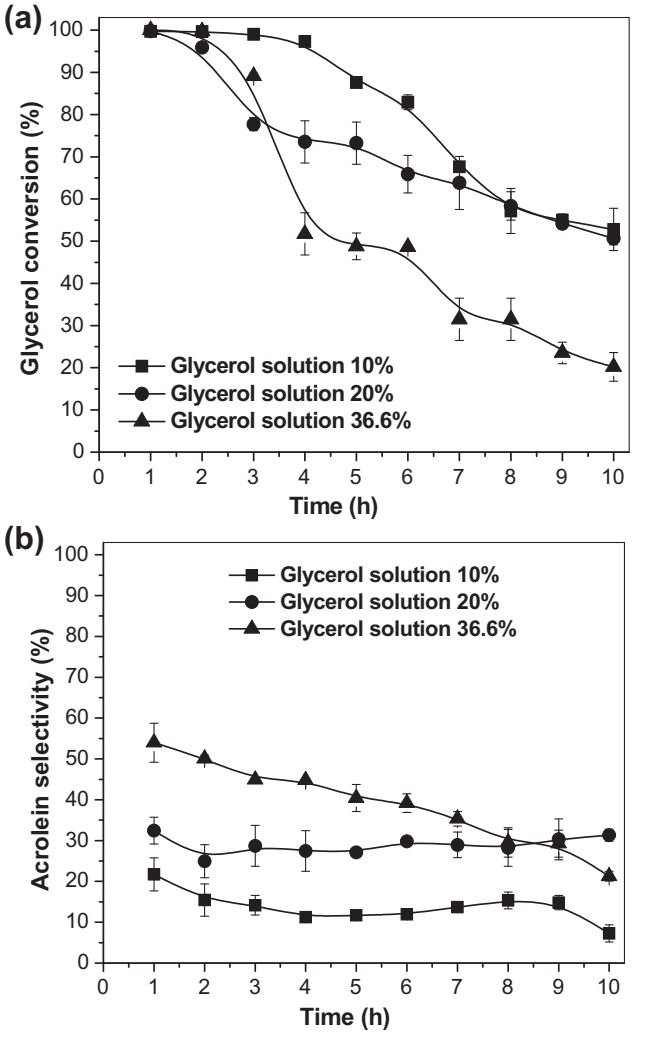

Fig. 9. Glycerol conversion and acrolein selectivity over MCM-22 (30) catalyst at different feed composition. Glycerol flow = 0.33 mL/min, T = 320 °C, catalyst weight = 0.10 g.

Table 5
The catalytic performance for the dehydration of glycerol over MCM-22 catalysts with different W/F ratio.[a,b]

Catalyst	MCM-22 (30)		
W/F (g s mmol^{-1})	20.8	41.6	125.0
Conversion (%)	99.46 (15.45)	99.75 (20.20)	95.23 (64.88)
Acrolein yield (%)	35.52 (2.33)	49.92 (4.30)	49.64 (25.00)
Molar selectivity (%)			
Acrolein	35.71 (15.07)	50.05 (21.28)	52.13 (38.54)
1-hydroxyacetone	1.58 (4.73)	2.04 (0)	3.66 (2.38)
Formaldehyde	1.61 (12.59)	4.60 (13.57)	4.98 (5.59)
Acetaldehyde	2.58 (17.32)	5.53 (15.28)	5.72 (7.30)
Acetone	0.23 (0.37)	0.15 (0.39)	0.25 (0.35)
Allyl alcohol	0.34 (0.40)	0.27 (0)	0.36 (0.05)
Propionic acid	3.78 (6.93)	4.21 (0)	1.41 (0.53)
Propionaldehyde	0.18 (0.99)	0.11 (0.74)	0.06 (0.07)
Others	51.99 (41.60)	33.04 (48.74)	31.43 (45.19)
Coke[c] (%)	20.78	24.61	27.24

[a] Feed composition: 36.6% glycerol, Glycerol flow = 0.33 mL/min, T = 320 °C.
[b] The conversion and selectivity were analyzed for the products obtained during the initial 2 h of reaction. Data in parenthesis were analyzed for the products obtained from 10 to 12 h of reaction.
[c] After the reaction for 12 h.

Table 6
The catalytic performance for the dehydration of glycerol over MCM-22 catalysts with different glycerol content.[a,b]

Catalyst	MCM-22 (30)		
Glycerol content (%)	10	20	36.6
Conversion (%)	99.67 (52.77)	95.91 (50.65)	99.75 (20.20)
Acrolein yield (%)	15.39 (3.83)	23.94 (15.87)	49.92 (4.30)
Molar selectivity (%)			
Acrolein	15.44 (7.26)	24.96 (31.34)	50.05 (21.28)
1-hydroxyacetone	0.86 (0.48)	1.60 (1.57)	2.04 (0)
Formaldehyde	2.99 (1.26)	4.16 (6.16)	4.60 (13.57)
Acetaldehyde	3.45 (1.93)	4.72 (7.15)	5.53 (15.28)
Acetone	0.17 (0.07)	0.23 (0.27)	0.15 (0.39)
Allyl alcohol	0.04 (0)	0.15 (0.02)	0.27 (0)
Propionic acid	0.22 (0.27)	0.44 (0.33)	4.21 (0)
Propionaldehyde	0.14 (0.24)	0.04 (0.10)	0.11 (0.74)
Others	76.69 (88.49)	63.70 (53.06)	33.04 (48.74)
Coke[c] (%)	16.29	20.38	24.61

[a] Feed composition: 36.6% glycerol in He; glycerol flow = 0.33 mL/min, T = 320 °C, catalyst weight = 0.10 g.
[b] The conversion and selectivity were analyzed for the products obtained during the initial 2 h of reaction. Data in parenthesis were analyzed for the products obtained from 10 to 12 h of reaction.
[c] After the reaction for 12 h.

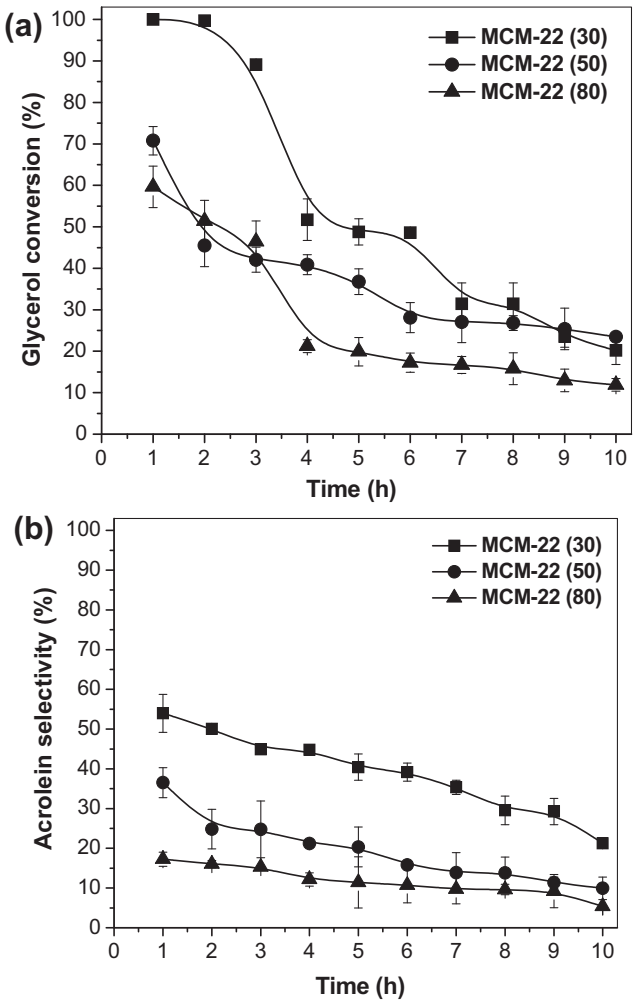

Fig. 10. Glycerol conversion and acrolein selectivity over MCM-22 catalysts with different molar ratio SiO_2/Al_2O_3. Feed composition: $T = 320$ °C; 36.6% glycerol; glycerol flow = 0.33 mL/min, catalyst weight = 0.10 g.

Table 7
The catalytic performance for the dehydration of glycerol over MCM-22 catalysts with different molar ratio SiO_2/Al_2O_3.[a,b]

Catalyst	MCM-22		
Molar ratio SiO_2/Al_2O_3	30	50	80
Conversion (%)	99.75 (20.20)	45.48 (23.46)	51.41 (11.88)
Acrolein yield (%)	49.92 (4.30)	11.29 (2.33)	8.24 (0.64)
Molar selectivity (%)			
Acrolein	50.05 (21.28)	24.83 (9.93)	16.02 (5.37)
1-hydroxyacetone	2.04 (0)	1.19 (1.17)	1.22 (2.24)
Formaldehyde	4.60 (13.57)	3.29 (2.62)	3.84 (8.80)
Acetaldehyde	5.53 (15.28)	4.38 (4.53)	4.49 (8.61)
Acetone	0.15 (0.39)	0.18 (0.11)	2.08 (0.74)
Allyl alcohol	0.27 (0)	0.09 (0)	0 (0)
Propionic acid	4.21 (0)	2.04 (2.08)	0.52 (0.82)
Propionaldehyde	0.11 (0.74)	0.26 (0.44)	0.35 (0.40)
Others	33.04 (48.74)	63.74 (79.12)	71.48 (73.02)
Coke[c] (%)	24.61	25.60	12.87

[a] Feed composition: 36.6% glycerol in He; glycerol flow = 0.33 mL/min, $T = 320$ °C, catalyst weight = 0.10 g.
[b] The conversion and selectivity were analyzed for the products obtained during the initial 2 h of reaction. Data in parenthesis were analyzed for the products obtained from 10 to 12 h of reaction.
[c] After the reaction for 12 h.

and selectivity to the products of the reaction are shown in Table 5. It was observed that higher W/F ratio also favors the formation of a larger amount of by-products and acrolein. Furthermore, it can also be related to the amount of coke formed, which modifies the nature of acid sites over the course of the reaction, favoring secondary reactions [28].

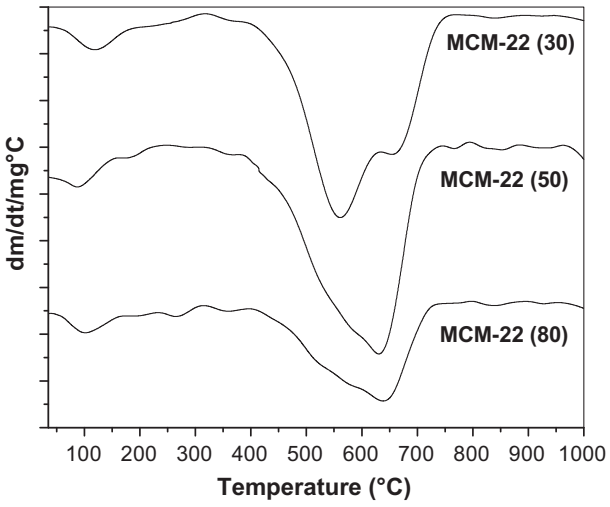

Fig. 11. Thermogravimetry of MCM-22 catalysts after 10 h of reaction.

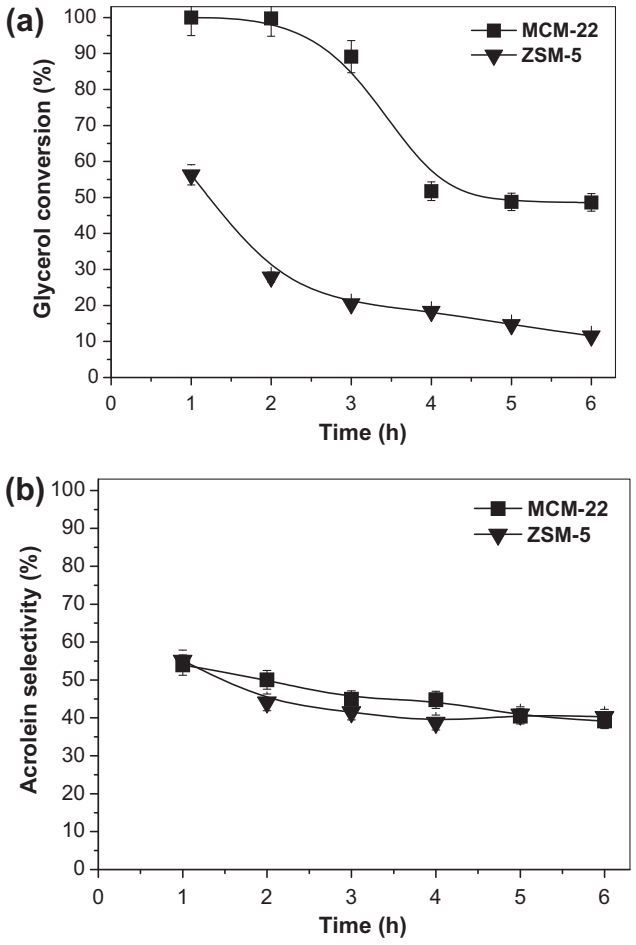

Fig. 12. Comparison of MCM-22 (30) and ZSM-5 (30) catalytic performances. Feed composition: $T = 320$ °C; 36.6% glycerol; glycerol flow = 0.33 mL/min, catalyst weight = 0.10 g.

3.2.3. Effect of glycerol content

The variation in glycerol content in the feed is showed in Fig. 9. As long as the concentration of glycerol solution was in the range from 10% to 36.6%, there was no noticeable difference in the glycerol initial conversion. The catalyst deactivation with the reaction time is more pronounced in the test performed with higher glycerol concentration, which promotes hydrogen transfer reactions and produce more coke [31] as shown in Table 6. At the end of reaction, the MCM-22 showed about 50% conversion in solutions of 10 and 20% of glycerol and approximately 20% of conversion in the solution containing 36.6% glycerol. In spite of lower glycerol concentration has favored higher conversions and slower deactivation by coke formation, these conditions do not present the best acrolein selectivities. The increase in glycerol content results in an acrolein selectivity increase.

3.2.4. Effect of molar ratio SiO_2/Al_2O_3

The influence of SiO_2/Al_2O_3 molar ratio on the glycerol dehydration to acrolein is shown in Fig. 10. The increase in molar ratio SiO_2/Al_2O_3 causes a decrease in glycerol conversion and acrolein selectivity. MCM-22 (30) showed a higher glycerol conversion and acrolein selectivity that can be explained by the highest amount of acid sites and external area of this zeolite. These results are consistent with literature data for other zeolite catalysts, particularly the zeolite ZSM-5, which result indicate that a high amount of acid sites and high external surface area contributes to the best results of glycerol conversion and acrolein selectivity [27].

The data showed in Table 7 indicate that the catalysts with an stronger acidity formed larger amount of carbonaceous residues than those with weaker acidity, indicating that acrolein molecules are easily subjected to secondary reactions due to the presence of coke [28]. It was also observed a high amount of non-condensable byproducts in reactions using MCM-22 (50) and MCM-22 (80) catalysts, which is in concordance with the lower acrolein selectivity of these materials.

The decrease in glycerol conversion suggests that there is coke formation in the channels and cages of the catalyst, blocking acid sites. X-ray diffraction analyses of the after test samples showed no significant changes in the zeolite structure during the reaction, but some increase in the amorphous halo can be seen, indicating that coke is segregated as an amorphous phase. The coke amount was determined by TGA/DTG in an oxidizing atmosphere for samples of zeolite MCM-22 with different SiO_2/Al_2O_3 molar ratios after 10 h of catalytic test. TGA curves are shown in Fig. 11 and the amount of coke, determined by mass loss in the region of 400–800 °C, are shown in Tables 4–7. These results confirm the formation of carbon deposits, which increased with decreasing SiO_2/Al_2O_3 ratio of the zeolite MCM-22, suggesting that coke formation is related to the amount of strong acid sites.

Three events of weight loss were observed by the coke burning: (i) around 550 °C, corresponding to thermally unstable coke, probably formed on the external surface of crystallites; (ii) at 640 °C, referent to the coke deposited on the MWW supercages or surface cups; and (iii) nearly 680 °C, relative to carbonaceous deposits in

Table 8
Comparison of catalytic performance of different zeolite catalysts in the gas phase dehydration of glycerol to acrolein.

Catalyst	SiO_2/Al_2O_3	T (°C)	W/F (g s mmol^{-1})	$\chi_{glycerol}$ (%)[a]	$S_{acrolein}$ (%)[b]	Refs.
H-ZSM-5	n.i.	315	6.35	80 (23)	36 (54)	[33]
H- β	n.i.	315	6.35	95 (60)	34 (43)	[33]
SAPO-34	n.i.	315	6.35	55 (32)	34 (48)	[33]
SBA-15	∞	315	6.35	71 (31)	29 (30)	[33]
SAPO-11	n.i.	280	2209	78 (18)	35 (18)	[34]
SAPO-34	n.i.	280	2209	45 (5)	47 (11)	[34]
H-ZSM-5[c]	n.i.	470	3.6	67.6	9.8	[35]
H-Y[c]	n.i.	470	18.1	95.8	15.4	[35]
H-ZSM-5	28	320	2.84	100 (68)	45 (45)	[30]
H-ZSM-5	36	320	2.84	100 (60)	60 (60)	[30]
H-ZSM-5	130	320	2.84	100 (100)	45 (60)	[30]
H-ZSM-5	290	320	2.84	15 (3)	7 (5)	[30]
Silicalite-1	∞	320	2.84	13 (5)	11 (3)	[30]
Na-ZSM-5	23	315	46.2	10.1 (3.4)	0.6 (1.1)	[12]
H-ZSM-5	30	315	46.2	51.9 (28.2)	41.6 (30.9)	[12]
H-ZSM-5	60	315	46.2	49.3 (16.5)	55.8 (37.7)	[12]
H-ZSM-5	150	315	46.2	75.8 (26.5)	63.8 (43.6)	[12]
H-ZSM-5	500	315	46.2	38.6 (13.9)	43.8 (32.0)	[12]
H-ZSM-5	1000	315	46.2	8.8 (≈0)	5 (≈0)	[12]
H-ferrierite	23	315	46.2	42.0 (19.8)	40.7 (37.5)	[27]
H-ferrierite	55	315	46.2	45.6 (11.6)	59.0 (46.8)	[27]
H-β	25	315	46.2	76.4 (28.9)	45.8 (34.1)	[27]
H-β	27	315	46.2	74.8 (34.0)	46.7 (39.5)	[27]
H-β	38	315	46.2	30.1 (6.0)	33.1 (23.9)	[27]
H-β	350	315	46.2	36.7 (4.6)	38.8 (17.1)	[27]
H-ZSM-5	23	315	46.2	36.3 (20.6)	45.8 (41.6)	[27]
H-Y	5.1	315	46.2	29.7 (13.2)	29.7 (29.6)	[27]
H-mordenite	20	315	46.2	49.5 (23.7)	40.5 (34.1)	[27]
H-Y[d]	12	320	203.4	46.6	35.5	[36]
Bulk H-ZSM-5[d]	31	320	203.4	71.8	42.2	[36]
Nano H-ZSM-5[d]	30	320	203.4	93.4	52.4	[36]
H-β[d]	26	320	203.4	69.5	38.9	[36]
H-ZSM-11[d]	50	320	203.4	89.7	53.4	[36]
H-ZSM-5[c]	42.8	320	41.6	27.9 (11.5)	44.1 (40.3)	This work
H-MCM-22	36.6	320	41.6	99.8 (20.2)	50.1 (21.3)	This work
H-MCM-22	47.2	320	41.6	45.5 (23.5)	24.8 (9.9)	This work
H-MCM-22	78.0	320	41.6	51.4 (11.9)	16.0 (5.4)	This work

[a] Glycerol conversion after 2 h (and 10 h) on stream.
[b] Acrolein selectivity after 2 h (and 10 h) on stream.
[c] TOS = 6 h.
[d] TOS = 3 h; n.i. = not informed.

the 10 MR channel. These results also indicate that coke can be removed, at least partially, by thermal treatment under oxidative atmosphere, suggesting that an industrial process should employ a two stage reactor, one where glycerol dehydration takes place and other, where catalyst would be regenerated by coke burning.

3.2.5. Comparison of MCM-22 with other zeolite catalysts

Zeolite ZSM-5 is the most studied catalyst for this reaction. In order to compare the efficiency of these catalyst under the same conditions, a sample was prepared by using the IZA method with nominal molar ratio $SiO_2/Al_2O_3 = 30$ [32], calcined and subsequently converted to its acid form following the same procedure previously described. The final material presented the following properties: $SiO_2/Al_2O_3 = 42.8$, $S_{BET} = 377\ m^2\ g^{-1}$, $V_{micro} = 0.101\ cm^3\ g^{-1}$, $V_{meso} = 0.039\ cm^3\ g^{-1}$, total density of acid sites = 0.42 mmol g^{-1}.

The comparison of catalytic performances of MCM-22 (30) and ZSM-5 (30) in the vapor phase dehydration of glycerol to acrolein is shown in Fig. 12. The MWW material presented higher glycerol conversion than ZSM-5, what can be attributed to the higher amount of total acid sites, besides the higher strong acid sites of MCM-22 sample. ZSM-5 also deactivated quickly in the first hour of reaction, because of the pore obstruction by coke formation, what is expected based on its textural properties and in MFI topology, which is formed exclusively by channels, while MWW topology has also supercavities. Acrolein selectivity is very similar for both catalysts, suggesting that MCM-22 produces a higher amount of by-products without loss in acrolein selectivity.

A comparison between the catalytic performance of MCM-22 and other zeolite in the literature is not straightforward, mainly because of the different experimental conditions employed to evaluate the different catalysts. However, the main catalytic performances found for zeolites in the literature were summarized in Table 8 and our comparison was done only with those papers with similar conditions of reaction temperature and W/F ratio.

As can be seen in Table 8, MCM-22 (30) has presented a better glycerol conversion than other zeolites evaluated under comparable experimental conditions [12,27]. Moreover, similar acrolein selectivities were observed when compared to H-ZSM-5 and H-ferrierite, but superior to those found for H- β, H-Y or H-mordenite. MCM-22 catalyst deactivation by coke formation is less significant during the early 6 h on stream when compared to literature catalyst, probably due to the contribution of acid sites located inside mesopores, but continues to deactivate in the last 4 h of reaction, what lead to higher coke deposits. Some results found in the literature seem to be better than those related in this work, however the W/F ratios used for catalyst evaluation were much more lower or higher than that used for MCM-22 tests.

4. Conclusions

MCM-22 zeolite proved to be active and selective in the gas phase dehydration of glycerol to acrolein. Highest glycerol conversions and selectivities to acrolein were observed for the catalyst with SiO_2/Al_2O_3 molar ratio = 30, which presents the highest amount of acid sites and surface area. The primary mechanism of catalyst deactivation is the blockage of the pores by the formation of carbonaceous deposits, which can be easily removed by burning in an oxidizing atmosphere.

Acknowledgement

The authors acknowledge the financial support from the National Council of Technological and Scientific Development (CNPq – no. 476657/2010-5).

References

[1] M.K. Rubin, P. Chu, US Patent No. 4954325, 1990.
[2] U. Diaz, V. Fornes, A. Corma, Microporous Mesoporous Mater. 90 (2006) 73–80.
[3] R. Ravishankar, D. Bhattacharya, N.E. Jacob, S. Sivasanker, Microporous Mater. 4 (1995) 83–93.
[4] S. Lawton, M.E. Leonowicz, R. Partridge, P. Chu, M.K. Rubin, Microporous Mesoporous Mater. 23 (1998) 109–117.
[5] M.R. Mihalyi, I. Kolev, V. Mavrodinova, C. Minchev, M. Kollar, J. Valyon, React. Kinet. Catal. Lett. 92 (2007) 345–354.
[6] Z. Sobalik, Z. Tvaruzkova, B. Wichterlova, V. Fila, S. Spatenka, Appl. Catal. A Gen. 253 (2003) 271–282.
[7] Y. Zhang, H.J. Xing, P.P. Yang, P. Wu, M.J. Jia, J.Z. Sun, T.H. Wu, React. Kinet. Catal. Lett. 90 (2007) 45–52.
[8] K. Okumura, M. Hashimoto, T. Mimura, M. Niwa, J. Catal. 206 (2002) 23–28.
[9] H.K. Min, M.B. Park, S.B. Hong, J. Catal. 271 (2010) 186–194.
[10] A. Corma, J. MartinezTriguero, J. Catal. 165 (1997) 102–120.
[11] J. Weitkamp, Solid State Ionics 131 (2000) 175–188.
[12] Y.T. Kim, K.D. Jung, E.D. Park, Microporous Mesoporous Mater. 131 (2010) 28–36.
[13] J. Wang, X. Tu, W. Hua, Y. Yue, Z. Gao, Microporous Mesoporous Mater. 142 (2011) 82–90.
[14] L. Xuemei, Z. Chunlei, Q. Chunhua, C. Chao, S. Jingming. CN 1010726A, 2007.
[15] A.L.S. Marques, J.L.F. Monteiro, H.O. Pastore, Microporous Mesoporous Mater. 32 (1999) 131–145.
[16] M.A. Camblor, C. Corell, A. Corma, M.J. Diaz-Cabañas, S. Nicolopoulos, J.M. Gonzalez-Calbet, M. Vallet-Regi, Chem. Mater. 8 (1996) 2415–2417.
[17] M.A. Camblor, A. Corma, M.J. Diaz-Cabanas, C. Baerlocher, J. Phys. Chem. B 102 (1998) 44–51.
[18] A. Corma, C. Corell, V. Fornés, W. Kolodziejski, J. Pérez-Pariente, Zeolites 15 (1995) 576–582.
[19] A. Corma, C. Corell, J. Pérez-Pariente, Zeolites 15 (1995) 2–8.
[20] Y.J. Wu, X.Q. Ren, Y.D. Lu, J. Wang, Microporous Mesoporous Mater. 112 (2008) 138–146.
[21] Y.J. Wu, X.Q. Ren, J. Wang, Mater. Chem. Phys. 113 (2009) 773–779.
[22] J. Rouquerol, F. Rouquerol, K.S.W. Sing, Adsorption by Powders and Porous Solids: Principles, Methodology and Applications, Academic Press, 1998.
[23] S.J. Gregg, K.S. Sing. Adsorption, Surface Area and Porosity, second ed., Academic Press, London, 1982.
[24] E.G. Derouane, C.D. Chang, Microporous Mesoporous Mater. 35 (2000) 425–433.
[25] M. Brandle, J. Sauer, J. Am. Soc. 120 (1998) 1556–1570.
[26] A. Biaglow, R.J. Gorte, D. White, J. Catal. 150 (1994) 221–224.
[27] Y.T. Kim, K.D. Jung, E.D. Park, Appl. Catal. A Gen. 393 (2011) 275–287.
[28] Y.T. Kim, K.D. Jung, E.D. Park, Appl. Catal. B Environ. 107 (2011) 177–187.
[29] A. Corma, G.W. Huber, L. Sauvanauda, P. O'Connor, J. Catal. 257 (2008) 163–171.
[30] C.J. Jia, Y. Liu, W. Schmidt, A.H. Lu, F. Schuth, J. Catal. 269 (2010) 71–79.
[31] S.G. Sastre, V. Fornes, A. Corma, J. Phys. Chem. B 104 (2000) 4349–4354.
[32] International Zeolite Association. International Zeolite Association.
[33] S.H. Chai, H.P. Wang, Y. Liang, B.Q. Xu, Green Chem. 9 (2007) 1130–1136.
[34] W. Suprun, M. Lutecki, T. Haber, H. Papp, J. Mol. Catal. 309 (2009) 71–78.
[35] K. Pathak, K.M. Reddy, N.N. Bakhshi, A.K. Dalai, Appl. Catal. A Gen. 372 (2010) 224–238.
[36] Y.L. Gu, N.Y. Cui, Q.J. Yu, C.Y. Li, Q.K. Cui, Appl. Catal. A Gen. 429 (2012) 9–16.